International Journal of Education, Science and Social Sciences

Original Research Article

Eco-Friendly Adsorbents for Removal of Heavy Metals and Rhodamine B Using Activated Rice Husk, Coconut Shell and Modified Clay

Gichuki G. John*, Okoth O. Maurice, Lutta T. Samwel and Lusweti K. John

Department of Chemistry & Biochemistry, School of Science, University of Eldoret, P.O. Box 1125-30100, Eldoret, Kenya

***Corresponding author's email:** jmwg2005@yahoo.co.uk

Received: 10th March, 2026, Accepted: 20th May, 2026, Published: 27th May, 2026

Abstract

Access to clean and safe drinking water requires effective filtration technologies. In the recent past, green adsorbents have gained attention as sustainable alternatives to conventional ones because they are derived from abundant, renewable, and naturally occurring materials or waste products. This study, therefore, investigated the preparation and application of activated rice husk charcoal (ARC), activated coconut shell charcoal (ACC), and acid-modified clay soil (ACS) as biosorbents for the removal of Co^{2+}, Cu^{2+}, Pb^{2+} ions, and rhodamine B (RB) dye from water. The adsorbents were characterized using FTIR, XRD, XRF, TEM, and BET before adsorption studies. Batch experiments were conducted to evaluate the effects of solution pH, temperature, contact time, particle size, and adsorbent dosage. Residual metal concentrations were quantified using Atomic Absorption Spectroscopy (AAS), achieving maximum removal efficiencies of 95%, 93% and 90% in ARC, 93%, 89% and 86% in ACC and 87%, 86% and 81% in ACS for Pb^{2+}, Cu^{2+} and Co^{2+}, respectively. For RB, 93%, 89% and 85% were achieved correspondingly by ARC, ACC and ACS, implying highest adsorption efficiency exhibited by ARC under the studied conditions. Metal ions removal was optimal at pH 6, whereas RB dye was highly adsorbed at pH 4. Overall, ARC, ACC, and ACS demonstrated significant

https://doi.org/10.69897

potential as eco-friendly adsorbents for the elimination of heavy metals and dyes from wastewater.

Keywords: Coagulation, degradation, heavy metals, functional groups, wastewater treatment, Langmuir isotherm, adsorption kinetics, biosorption

Introduction

The reality that the Earth is experiencing a wide range of severe environmental issues is widely documented. These issues include air pollution (Al-Sareji *et al.*, 2021) climate change (Salah *et al.*, 2018), and the generation of solid waste (Abdulredha *et al.*, 2017). But given the scarcity of freshwater resources on Earth, the biggest problem is water pollution (Al-Hashimi *et al.*, 2021). According to Yagub *et al.* (2014), there has been significant environmental degradation as a result of the growing use of dyes in numerous industries, including textiles, pharmaceutical, food, paper, and leather.

Light and informal (jua kali) businesses such as those that produce textiles, leather goods, paper goods, plastics, cement, metalworking, wood preservatives, paints and pigments, and steel fabrication have experienced a notable surge in growth. These industries discharge large quantities of poisonous wastes to water bodies making water unhealthy for domestic use (Chengo *et al.*, 2013).

Developing nations feel this scarcity most acutely due to unregulated industrial growth. Studies have shown that the open-air mechanical workshops are significant sources of mobile and bioavailable heavy metal contaminants (Chengo *et al.*, 2013). Several studies suggest that among the heavy metals, pollution associated with lead ions is of key concern (Muiruri *et al.,* 2013). Lead is a non-essential element and poisonous even at very low concentration resulting to impairment of nervous system (Tong *et al.*, 2000). People have been reported to suffer from nausea and vomiting at a level of 15 mg/L of lead, but with no negative impacts at 0.05 mg/L (Levin *et al.*, 2008).

Heavy metals are environmental priority pollutants and are becoming one of the most serious environmental problems. Therefore, toxic heavy metals should be removed from the wastewater to protect people and the environment. Many methods are being used to eliminate heavy metal ions as mentioned earlier (Fu and Wang, 2011). Currently the common methods available for elimination of metal ions from wastewater are coagulation, chemical precipitation, ion-exchange, reverse osmosis, among others (Hui *et al.*, 2005). However, most of these methods suffer from some drawbacks, such as high capital and operational costs or the disposal of the residual metal sludge (Kobya *et al.*, 2005).

Therefore, it is imperative to develop a system that is highly selective, more effective, simple to use, and consequently economical. Adsorption may be a useful substitute method for removing heavy metals such as Pb, Cu and Co and dyes such

https://doi.org/10.69897

as rhodamine B particularly in cases where the concentration is low. Adsorbent surface area, surface shape, pore size distribution, polarity, and functional groups affixed to the adsorbent surface all affect adsorption effectiveness (Ewecharoena *et al.*, 2009).

Agricultural waste is a readily available, abundant natural resource and a significant source of inexpensive adsorbents. Moreover, improper disposal of agricultural wastes results in major issues and low economic value. Utilizing agricultural wastes has two benefits. One is for the environment, turning undesirable, excess agricultural waste that was improperly disposed of by burning it into valuable adsorbents with additional value, while the other is for financial gain. Utilizing agricultural waste materials reduces the expensive preparation costs of the finished adsorbents (Ngah & Hanafiah, 2008). Few studies compare multiple low-cost adsorbents for simultaneous removal of heavy metals and dyes under identical conditions.

Materials and Methods

All reagents (≥ 98.5%) were analytical grade.

Instrumentation

After adsorption, Cu^{2+}, Pb^{2+}, and Co^{2+} ions were measured using an air-acetylene flame and a flame atomic absorption spectrophotometer. Using a pH meter (pH 211 microprocessor, Hanna instruments), the impact of pH on metal ion adsorption was ascertained. Activated carbon's organic functional groups that were in charge of the adsorption of heavy metal ions were identified using a Fourier transform infrared (FTIR) spectrophotometer (Model FTS-8000, Shimadzu, Japan).

Preparation of the adsorbents

Preparation of Coconut Shell and Rice Husk Charcoal

The raw materials were coconut shells and rice husks which were collected from coconut growing areas in the Kenyan coast and rice growing area of Mwea in Kirinyaga County, Kenya. The samples were sun dried, broken using a jaw crusher and then heated with limited supply of oxygen, at varying temperature profiles (from 600 to 1000 ^{0}C) in a furnace for two hours. The charcoal was allowed to cool and then rinsed with distilled water to remove impurities and fine dust. It was dried in an oven at 100 ^{0}C until a constant weight was achieved, before cooling again in a desiccator. It was crushed a second time and thereafter underwent particle size grading and screening. It was then sorted into sizes 18, 20 and 60 mesh using screens. It was then activated with steam and carbon dioxide to increase the surface area and stored in a sealed glass container until use.

https://doi.org/10.69897

Preparation of Clay

The unmodified bentonite clay was sourced from Isinya area, Kenya. To increase the functional group concentration, it was treated with 1 M hydrochloric acid (HCl), sulphuric acid H_2SO_4) and sodium hydroxide (NaOH) in the ratio of 1 g clay to 50 mL solution separately. The mixture was then shaken at speed of 120 rpm for 24 hours using an electrical shaker, and then washed with distilled water until a pH of about 6-7 was obtained. The modified clay then was separated from water by vacuum filtration, dried at room temperature, milled and finally sieved to obtain the average size of 0.074 mm in powder form. The modified and unmodified clays were characterized for their porous properties by nitrogen adsorption at 77 K.

Metals Solution Preparation

Analytical grade substances were all employed in this investigation. In a 1000 mL volumetric flask, 1.60 grams of $Pb(NO_3)_2$ were dissolved in distilled water to create stock solutions of lead (1000 mg/L), and water was then added to the appropriate level. 4.93 grams of $Co(NO_3)_2.6H_2O$ were dissolved in 1000 mL distilled water to make the cobalt ions stock solution. A 3.76 grams of $Cu(NO_3)_2.3H_2O$ were dissolved in distilled water to make a stock solution of copper, 1000 mg/L. The solution was then topped off with 1000 mL distilled water. Working solutions were made by serially diluting stock solutions with distilled water to achieve the proper dilutions.

Preparation of Dye Solutions

Stock solution was prepared by dissolving accurately weighed dye in known volume of distilled water. Serial dilutions were made by diluting the stock solutions in accurate proportions to the desired initial concentrations. The pH of each solution was adjusted with 0.5 M HCl and 1.0 M NaOH using a pH meter. Adsorption tests were conducted in a rotary shaker (150 rpm) using 250 mL flasks containing 100 mL of dye solutions of different concentrations at various initial pH values.

Batch Adsorption Experiments

Batch experiments were used to study sorption. In order to conduct the experiments, 50 mL water solutions with known concentrations of lead, cobalt, and copper were added to 150 mL conical flasks that had a known mass of adsorbent. Temperature-controlled agitation of test solutions was done at 120 rpm. The test solution's pH was brought to the appropriate ranges by adding sodium hydroxide and hydrochloric acid. Each solution was supplemented with 1.0 g of ACC, ARC, and ACS, mixed, and allowed to equilibrate. AAS was then used to measure the amounts of the Cu^{2+}, Co^{2+}, and Pb^{2+} ion filtrates after shaking the solution.

https://doi.org/10.69897

Adsorbent Characterization

Using Empyrean, PANalytical X-ray diffractometer with CuKα radiation, the crystalline structures of coconut shell and rice husk charcoal and clay were ascertained using X-ray diffraction (XRD) analysis. The diffraction patterns were obtained between diffraction angles of 0° to 90^0. FTIR was used to identify the functional groups that could have an impact on the adsorption process (a PerkinElmer 2000 FTIR spectrometer). Plotting the volume adsorbed (cm^3/g STP) against relative pressure (P/Po) revealed the BET surface area, average pore volume, and size distribution of the raw adsorbent. The adsorbents' chemical makeup was ascertained through the application of XRF analysis technology. The Empyrean, PANalytical XRF spectrometer with 60 kV energy of the X-ray tube was used to evaluate all samples and data were analyzed using AAS.

Experiments on Adsorption

Batch adsorption procedures were employed on dried coconut shells, rice husk charcoal, and clay by varying the temperature, adsorbent dosage, contact time, and solution pH. Adsorption investigations were carried out by adding 5.0 g of the adsorbent to 50 mL of aqueous metal solutions containing 1 ppm Co^{2+}, Cu^{2+}, and Pb^{2+} ions in solutions, respectively, and RB dye in conical flasks placed on a shaker in order to attain the equilibrium period. The effectiveness of metal ion and dye removal was investigated in relation to changes in solution temperature (273–373 K), adsorbent dosage (1, 2 and 5 g), contact duration (30, 60, 90, 120, 150, and 180 minutes), and pH (2–12). The quantities of metal ions and dyes were examined after filtration via a Whatman 42 filter.

The percent dye sorbed by the adsorbent at a given temperature, initial dye concentration, initial pH, adsorbent dose, ionic strength (when salts are added) and the duration of contact, was calculated in each case using the equation below:

$$\% \text{ removal} = ((C_i - C_e) / C_i) \times 100$$

where C_i (mg/L) and C_e (mg/L) are the initial and equilibrium concentrations of the dye, respectively. The experiments were conducted in duplicate and the negative controls (with no sorbent) were simultaneously carried out to ensure that sorption was by the adsorbent material and not by the container.

Results and Discussion

Characterization of the adsorbents

The active groups and bonds involved in the adsorption of metals onto the adsorbents were determined using FTIR spectroscopy. Numerous absorption peaks were visible in the FTIR spectra of ARC, ACC, and ACS, indicating the complex nature of the adsorbents. The existence of -OH groups in silanols (Si-OH) and siloxanes (Si-O-Si-OH) was revealed by the distinctive peaks at 3218 cm^{-1}, 3017 cm^{-1}, and 3380 cm^{-1}. This was further supported by the strong absorption at 1058 cm^{-1}, 1020 cm^{-1}, and 990 cm^{-1}, respectively, which demonstrated a Si-O asymmetric stretching. This

https://doi.org/10.69897

was in line with what Vieira *et al.* (2013) observed. The unsaturated C-C groups exhibited vibrational peaks at 2460 cm^{-1}, 2424 cm^{-1}, and 2446 cm^{-1}, in addition to peaks at wavelengths of 2159 cm^{-1}, 2152 cm^{-1}, and 2159 cm^{-1}. The peaks at 778 cm^{-1}, 795 cm^{-1}, and 756 cm^{-1} were caused by symmetrically stretched Si-H vibrations. The existence of alkenes and aromatic functional groups was revealed by the C=C stretching vibrations at 1600 cm^{-1}, 1557 cm^{-1}, and 1625 cm^{-1}. The C-H stretching vibration was associated with the peaks at around 2924 cm^{-1}, as reported by Bakti and Gareso (2018). The peaks demonstrated the adsorbent's complexity and its capacity to adsorb heavy metal ions and dye (Khan *et al.*, 2017).

Clay is crystalline, but rice and coconut activated charcoals are amorphous, according to XRD patterns of the adsorbents. The creation of groups and functions on the surface during preparation, along with the breakage of some C-C bonds (mostly those of the aromatic rings), account for the observed amorphism as shown in **Figure 1** (Zhao and Lang, 2018).

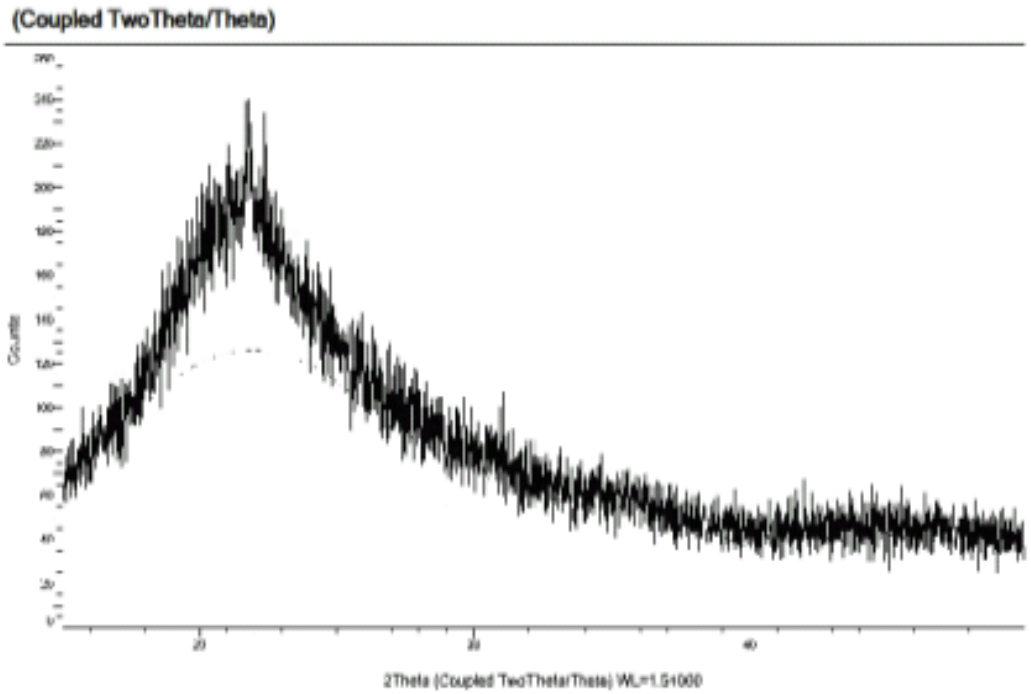

Figure 1: XRD image for ARC

The elemental makeup of adsorbents was examined using the XRF spectrometer. **Table 1** displays the results for ARC, ACC, and ACS. It's noteworthy that none of the three adsorbents contained lead, copper, or cobalt. In order to prevent them from interfering with the experiment, this needed to be confirmed. These results indicate that the primary components are SiO_2, Al_2O_3, and K_2O, with SiO_2 predominating particularly in ARC and ACS.

https://doi.org/10.69897

Table 1: Chemical composition (wt.%) for the adsorbents

	MgO	AL_2O_3	SiO_2	P_2O_5	S	Cl	K_2O	CaO	Ti	Cu	Co	Pb
ACC	0.00	2.11	4.30	5.76	2.31	3.58	65.48	11.04	1.21	0.00	0.00	0.00
ARC	0.00	0.34	94.26	0.78	0.13	0.05	2.00	1.55	0.09	0.00	0.00	0.00
ACS	6.07	14.14	63.90	0.02	0.31	0.03	6.45	2.17	0.56	0.00	0.00	0.00

Since XRD patterns for ACS samples differ from those for ACC and ARC, samples from all three adsorbents were selected for use in TEM investigation. The morphologies of these nanostructures differ greatly from one another. Although there were variations, a highly porous and hollow structure was always apparent, as shown in Figure 2, which is consistent with research done by Fu *et al.* (2011). The ARC was found to be composed of 10-15 nm grains, which were smaller than those for the ACC's (20–25 nm) but larger than the ACS's (25–30 nm) grains. ARC could have a larger surface area than ACC due to its smaller grains and many pores. According to Winter and Brodd (2004), the adsorbent in ACS is polycrystalline due to the presence of grains oriented in diverse orientations, but the adsorbent in ACC and ARC is amorphous due to unclear granules.

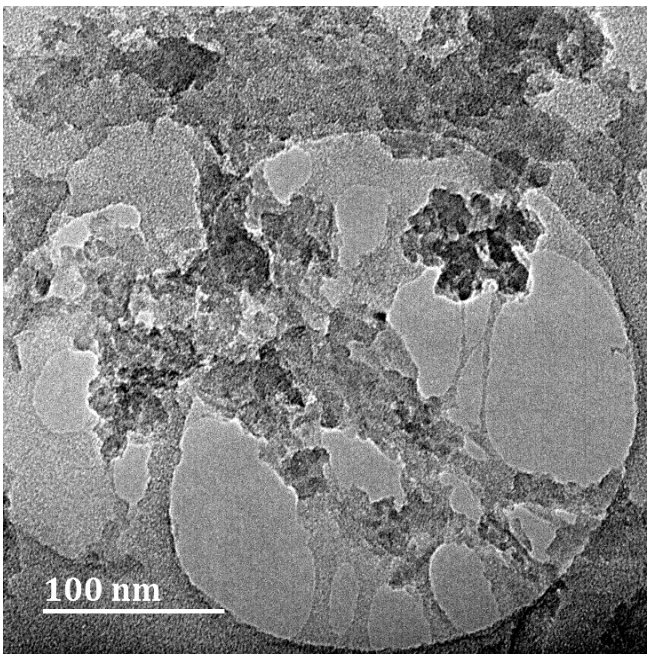

Figure 2: TEM image for rice husks adsorbent

Table 2 shows the surface area, micropore area, micropore volume and external surface area of the adsorbents.

https://doi.org/10.69897

Table 2: **The BET surface area, micropore area, micropore volume and external surface area**

Adsorbent	BET surface area (m^2/g)	Micropore area (m^2/g)	Micropore volume (cm^3/g)	External surface area (m^2/g)
ARC	72.0123	28.6609	0.008667	43.3515
ACC	1.1818	1.7029	0.000551	1.7029
ACS	0.2577	0.5300	0.000143	0.5300

The Effect of pH on Cu^{2+}, Co^{2+} and Pb^{2+} Ions and RB Percentage Removal

One important factor that is said to affect the adsorption process is the pH of an aqueous solution. The binding of metal ions onto the adsorbent during this process is often attributed to the functional groups, surface charges, degree of ionization, and solubility of the adsorbent. There is a net positive charge in the system at low pH levels because of the existence of H^+ and H_3O^+ ions. Due to intense competition for accessible sites on the adsorbent surface, this results in a high rate of partial discharge of metal cations (Sheta *et al.*, 2003). An increase in surface negative charges accompanied by a rise in pH facilitates the adsorption of metal ions (Gong *et al.*, 2005; Katircioğlu *et al.*, 2008). Adsorption works best at a moderate pH of 6 for the elimination of Cu^{2+}, Pb^{2+}, and Co^{2+} ions in all the three adsorbents, ARC, ACC and ACS, respectively as shown in **Figures** 3, 4 and 5 below.

Maximum metal ions removal was shown to occur in acidic media, and precipitates formed when pH levels were raised over their optimal range. Less adsorption occurred at lower pH levels because the adsorbent became protonated and the protons competed with the metal ions. Higher pH levels resulted in an increase in the interaction between these metal ions and the presence of negatively charged functional groups like hydroxyl ions, which ensured the development of the metal hydroxyl complex and affected the adsorption of metal ions onto the adsorbent. The creation of the metal hydroxyl complexes is caused by the electrostatic contact between the positively charged metal ions and the negatively charged hydroxyl ions, a monodentate ligand (Mustapha *et al.*, 2019). The binding of various metal ions to biomaterials with distinct functional groups in competitive systems is contingent upon the ionic characteristics of these metals, including their electronegativity, ionic radius, potential, and redox potential (Naja *et al.,* 2010). The competitive selective adsorption between ions is related to the hydration radius and electronegativity of heavy metals (Pang *et al.,* 2018). From **Figures 3** to **5**, it was noted that cobalt was the most adsorbed followed by copper and lead was the least. The assertion that larger ionic particles are less adsorbed than smaller ones is supported by this observation as well. The radius of hydrated metal ions affects adsorption selectivity, whereby the smaller the radius of hydrated metal ions, the less they are adsorbed by the adsorbent. Thus, Co^{2+} was more dominant in competitive adsorption.

https://doi.org/10.69897

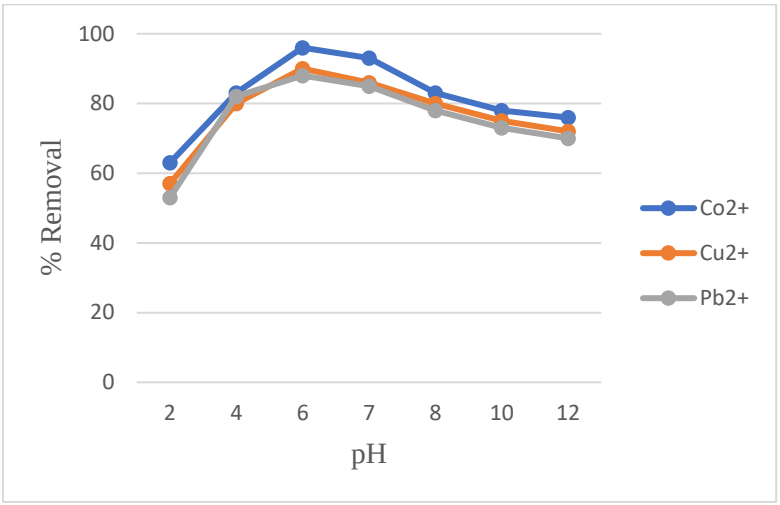

Figure 3: Effect of pH on metal ions percentage removal using ARC

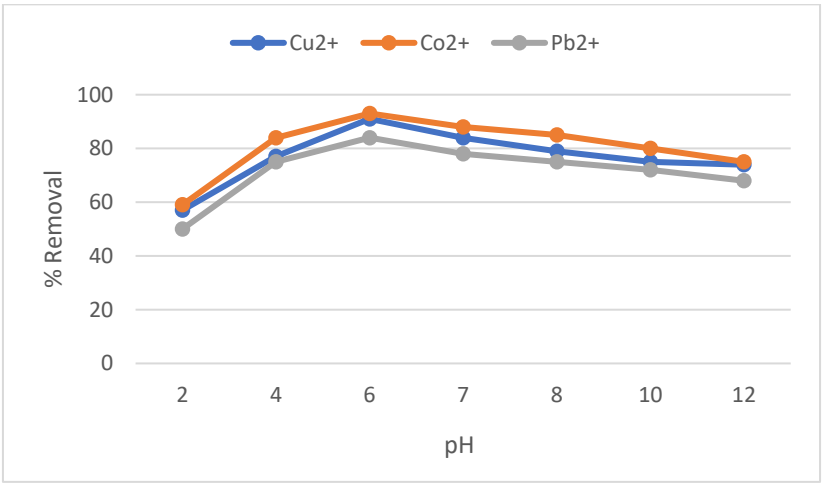

Figure 4: **Effect of pH on metal ions percentage removal using ACC.**

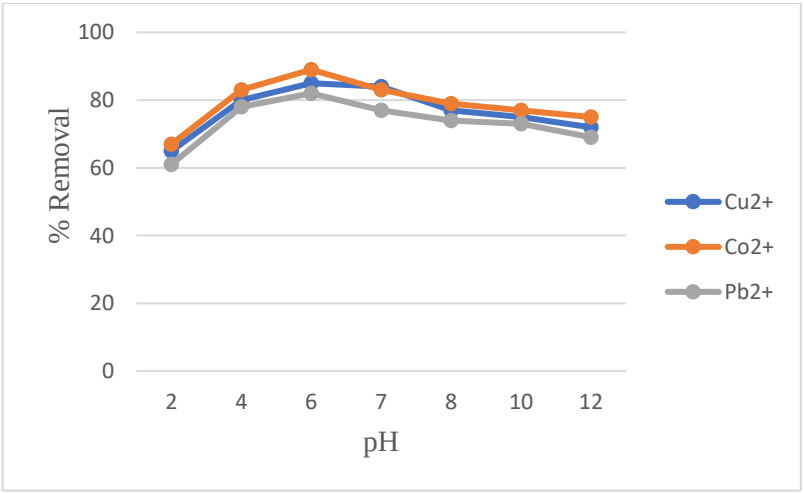

Figure 5: **Effect of pH on metal ions percentage removal using ACS.**

https://doi.org/10.69897

The effect of solution pH on RB sorption was studied using 5.0 g of ARC, ACC and ACS, 50 mg/L dye initial concentration, pH 2 to 12 at 25 ^{0}C and the results are shown in **Figure 6.**

The maximum equilibrium sorption capacity was obtained at pH 4 (75 %, 84 % and 90 % for ACS, ARC and ACC, respectively). For pH ranging from 4 to 8, the quantity of RB sorbed decreased gradually. In this pH range, the surface of sorbent was negatively charged resulting RB to exist as a zwitterion. At a pH value higher than 3.7, the zwitterionic form of RB in water could increase the aggregation of RB to form a larger molecular form (dimer) and become unable to enter through the pore. The greater aggregation of the zwitterion could be due to the attractive electrostatic interactions between the carboxyl and xanthene groups of the monomers (Ghanadzadeh *et al.,* 2002).

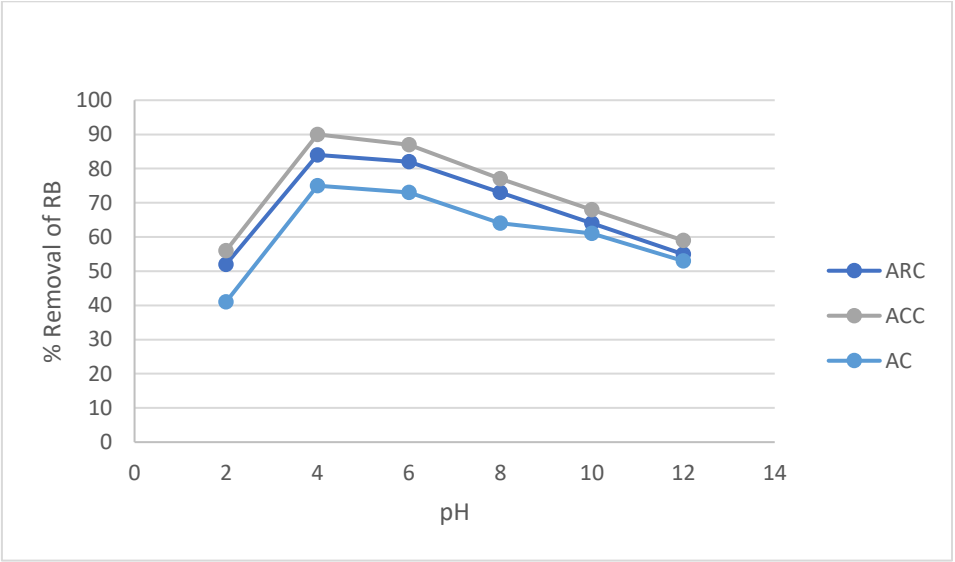

Figure 6: Effect of pH on RB percentage removal using 5.0 g of ARC, ACC and ACS

In comparing the three adsorbents, ARC had the highest adsorbent capability followed by ACC and finally ACS. This could be explained in terms of surface area, pore size and pore volume. ARC possessed the highest surface area and high adsorption capacity as compared to ACC and ACS. This is well confirmed in the BET analysis in **Table 2**.

Effect of Temperature

The temperature of the solution rose from 273 to 373 K, increasing the amount of adsorbate adsorbed per unit mass of adsorbent as shown in **Figure 7**. This increase illustrates the adsorption process' nature. The result shows that when the temperature rose, RB dye molecules were more mobile on an adsorbent. As the temperature of the solution varied, the kinetic energy of the dye molecules

https://doi.org/10.69897

increased, leading to an increase in the dye's mobility. The rise in temperature improved the adsorbent's pores, which ultimately made it easier for the adsorption process to occur spontaneously. Chemical interaction between RB and adsorbents was also observed at higher temperature which resulted in the creation of higher affinities between the active sites and RB dye. More so, when temperature was changed, it altered the adsorbent equilibrium capacity (Gupta *et al.,* 2012).

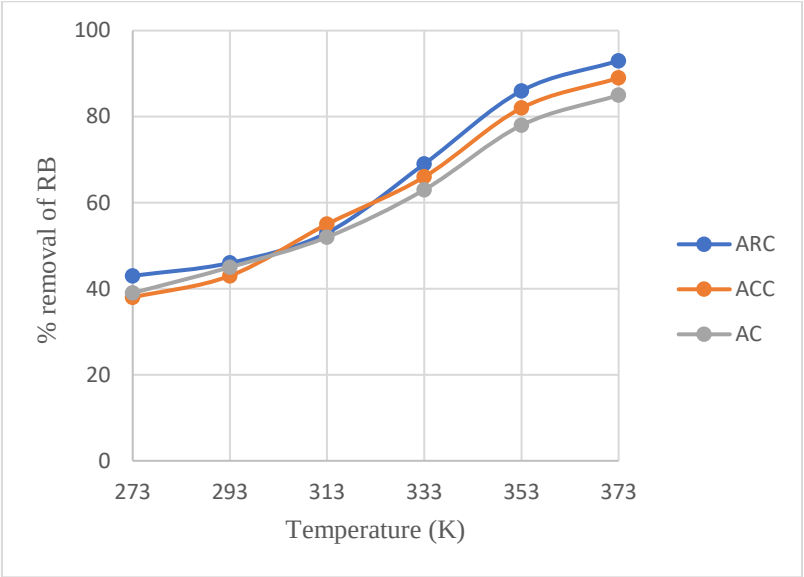

Figure 7: Effect of temperature on adsorption of RB with ARC, ACC and AC

Figures 8 to **10** show how temperature affects the adsorption of Pb^{2+}, Cu^{2+} and Co^{2+} ions.

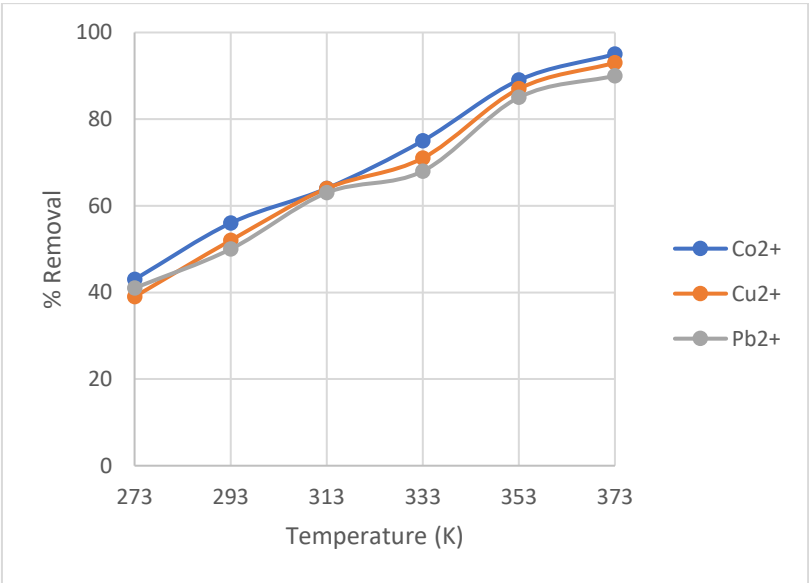

https://doi.org/10.69897

Figure 8: **Effect of temperature on metal ions percentage removal using ARC**

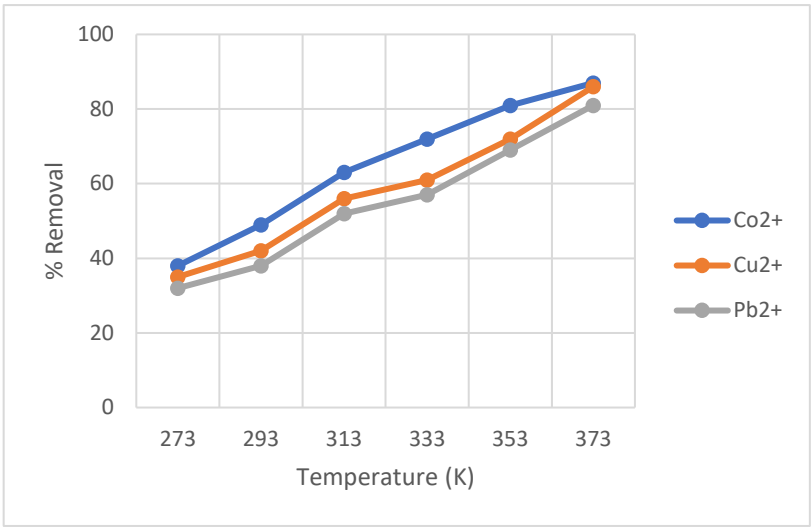

Figure 9: Effect of temperature on metal ions percentage removal using ACC

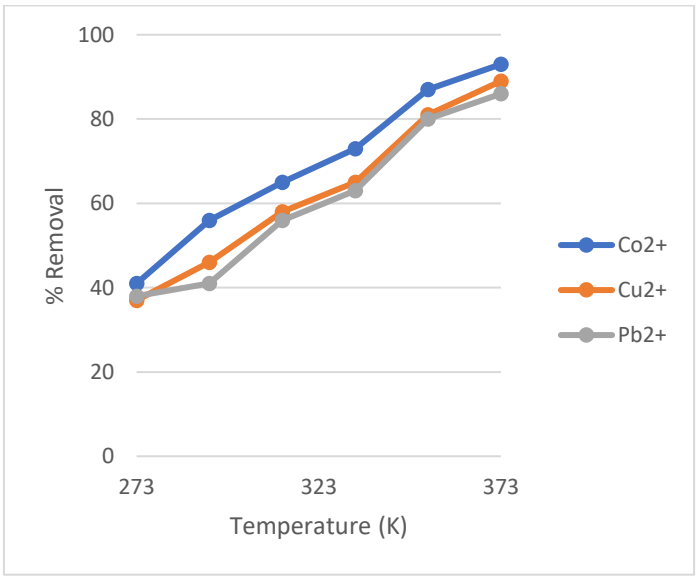

Figure 10: Effect of temperature on metal ions percentage removal using ACS

The adsorption capacity was observed to increase with increased temperature. This trend could be attributed to an increase in the frequency of reaction as the average velocity and metal ions diffusion increased and adhered to the adsorbent's surface (Manyangadze *et al.*, 2020). The maximum adsorption rate regarding the three metal ions within the three adsorbates was found to be between 333 K and 353 K because the increase in temperature favoured the adsorption equilibrium. The three metals' process of adsorption indicated to be endothermic in nature. This is because the surface particles on adsorbents surface were unstable

https://doi.org/10.69897

and when the metal ions were adsorbed, the energy of the adsorbents decreased resulting in the absorption of heat. Similar results were observed by Manyangadze *et al.* (2020) and Ugwu *et al.* (2020). In all adsorbents Co^{2+} ions were the most adsorbed more so in ARC with 95 % as compared to Pb^{2+} and Cu^{2+} with 90 % and 93 %, respectively as indicated in **Tables 3** to **5**.

Table 3: Effect of temperature on metal ions percentage removal using ARC

Temp (k)	Co^{2+}	Cu^{2+}	Pb^{2+}
273	43	39	41
293	56	52	50
313	64	64	63
333	75	71	68
353	89	87	85
373	95	93	90

Table 4: Effect of temperature on metal ions percentage removal using ACC

Temp (k)	Co^{2+}	Cu^{2+}	Pb^{2+}
273	41	37	38
293	56	46	41
313	65	58	56
333	73	65	63
353	87	81	80
373	93	89	86

Table 5: Effect of temperature on metal ions percentage removal using ACS

Temp (k)	Co^{2+}	Cu^{2+}	Pb^{2+}
273	38	35	32
293	49	42	38
313	63	56	52
333	72	61	57
353	81	72	69
373	87	86	81

As the average velocity and diffusion of metal ions rose and stuck to the adsorbent's surface, this trend might be explained by the size of the ion and an increase in the rate of reaction (Manyangadze *et al.*, 2020).

Effect of Shaking Speed

Adsorption resulted in high selectivity for Co^{2+} over all other available ions, thus $Co^{2+} > Cu^{2+} > Pb^{2+}$, with all adsorbents having above 80 % removal efficiency at the speed between 200 and 250 revolutions per minute as shown in **Figures 11** to **13**. This improvement in Co^{2+} adsorption could be due to its higher ionic potential and reduced size, which may result in a faster diffusion and stronger

https://doi.org/10.69897

adsorption as an outcome of the acidic groups located at the pore edges. Therefore, it will repel and hinder other ions from accessing the activated carbon pores (Irannajad and Haghighi, 2017).

Accordingly, increasing the shaking speed increases the diffusion of metal ions towards the adsorbent's surface because it releases more kinetic energy, which weakens the bonds between the Pb^{2+}, Cu^{2+}, and Co^{2+} ions in solution and the binding sites. This makes the binding sites more accessible and speeds up the rate at which sorbate ions are transferred to the sorbent sites (Argun *et al.*, 2006). A 200 rpm was found to be the ideal speed for shaking in order to guarantee that cell surfaces for binding sites are available for the adsorption process to proceed Pb^{2+}, Cu^{2+} and Co^{2+}.

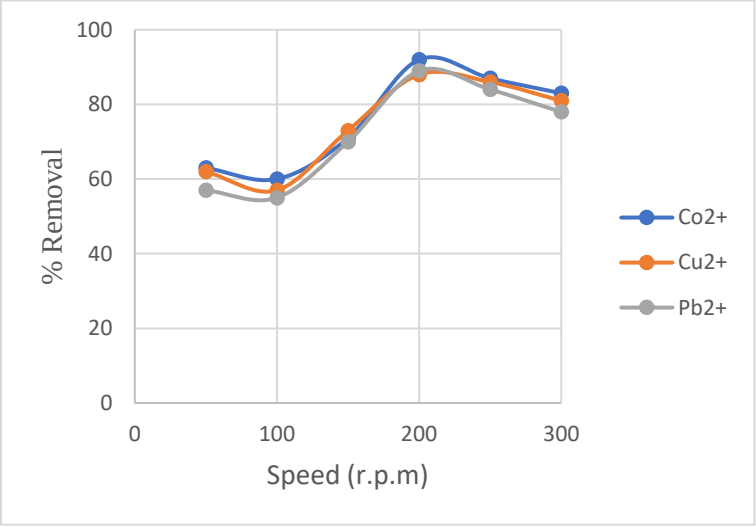

Figure 11: Effect of the shaking Speed on the Adsorption of metal ions in ARC

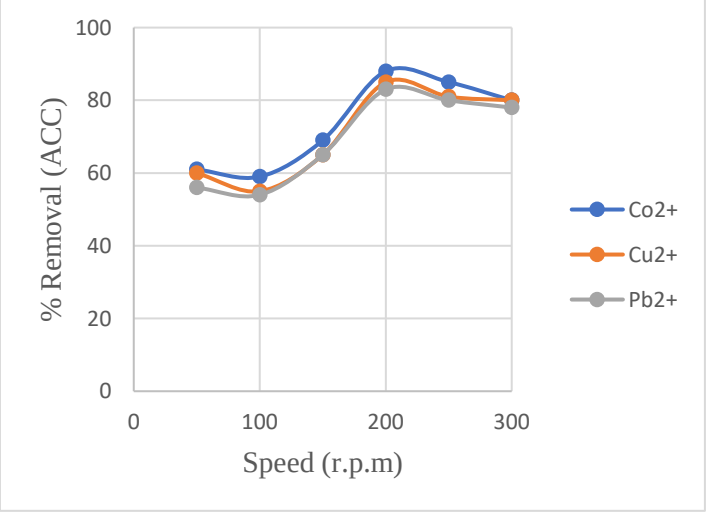

https://doi.org/10.69897

Figure 12: Effect of the shaking Speed on the Adsorption of metal ions in ACC

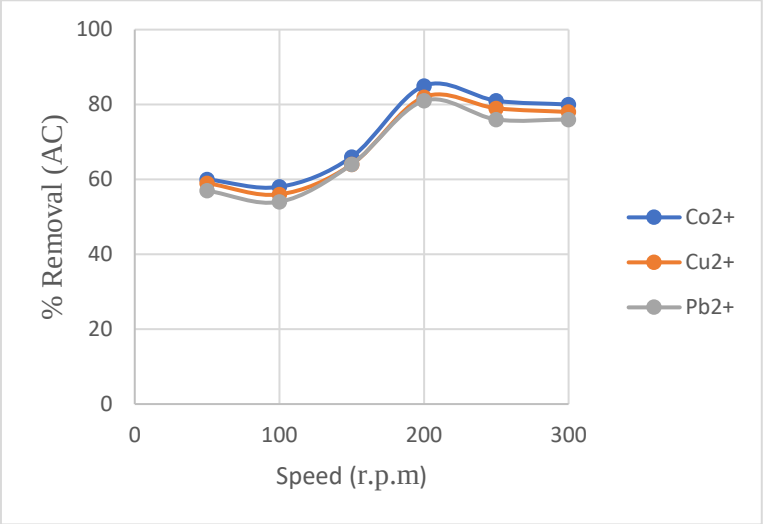

Figure 13: Effect of the shaking Speed on the Adsorption of metal ions in ACS

Effects of contact time

Impact of contact duration on the elimination of the dye Rhodamine B is illustrated in **Figure 14** and **Table 4**. It demonstrates that the elimination of the dye increased with contact time and it was rapid initially up to 40 minutes, then it proceeded at slower rate and finally almost attained saturation. This behaviour indicates that the adsorbate was rapidly adsorbed on its exterior during the first stage, which may have been the rate-determining phase. Eventually this stage was then followed by a slower interior diffusion process.

https://doi.org/10.69897

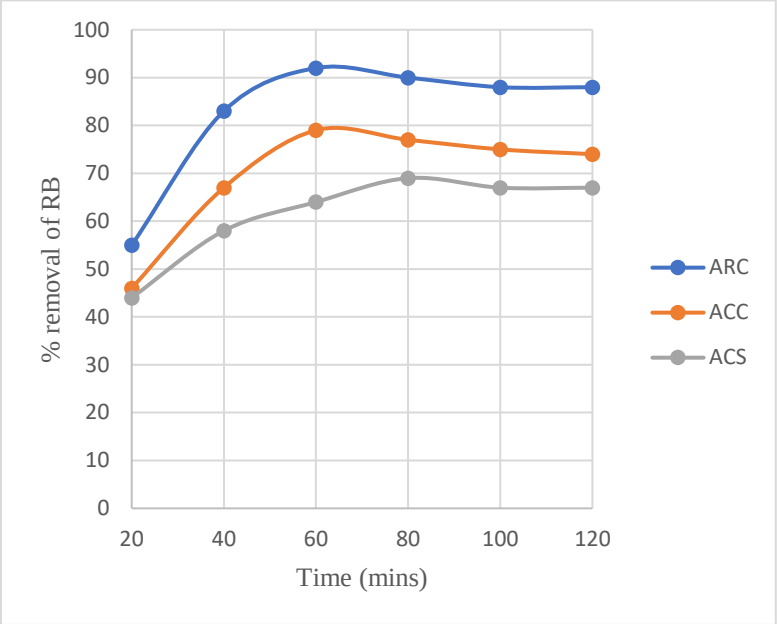

Figure 14: Effect of contact time on adsorption of RB with ARC, ACC and ACS

Table 4: Effect of contact time on adsorption of RB with ARC, ACC and ACS

Time (mins)	ARC	ACC	ACS
20	55	46	44
40	83	67	58
60	92	79	64
80	90	77	69
100	88	75	67
120	88	74	67

Adsorption rate increased quickly at first, reaching the ideal removal efficiencies of 58, 67, and 83 % for ACS, ACC, and ARC, respectively, after around 40 minutes. However, with adsorption rates of 79, 92, and 69%, respectively, the equilibrium (maximum) value was reached at about 60 minutes for ACC and ARC and 80 minutes for ACS. Additionally, after equilibrium was attained, the removal efficiencies dropped by roughly 2 to 5 % with longer contact times which suggests a physical adsorption (physisorption) component where the bond is weak enough for ions to detach once the surface energy changes. This most likely happened as a result of the dye being saturated on the adsorbent surfaces, which was followed by the adsorption and desorption processes (Argun, *et al.,* 2006). It was determined from **Figure 14** that ARC was always a superior adsorbent. Its large surface area in comparison to the other two, as indicated in **Table 4**, could be the cause of this. Therefore, adsorbents for RB were found to be in the order: ARC>ACC>ACS. This was consistent with the surface area of the BET. The impact of contact duration on

https://doi.org/10.69897

the adsorbents' ability to absorb Pb^{2+}, Cu^{2+}, and Co^{2+} ions is depicted in **Figures 15** to **17**. In different experimental runs, the contact period was varied from 20 to 120 minutes to achieve this.

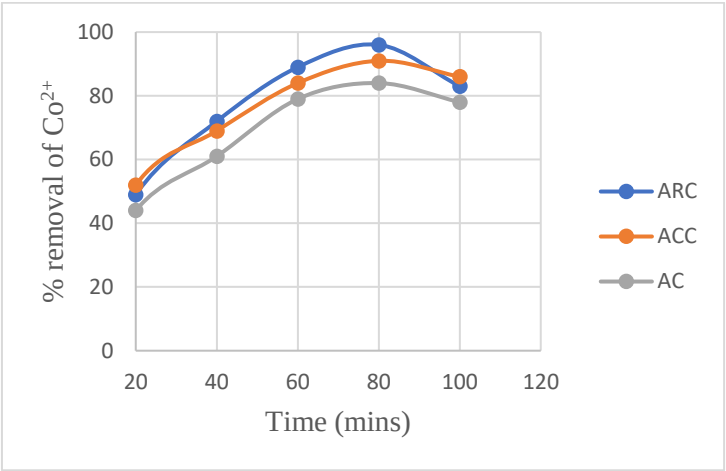

Figure 15: Effect of contact time on adsorption of Co^{2+} with ARC, ACC and ACS

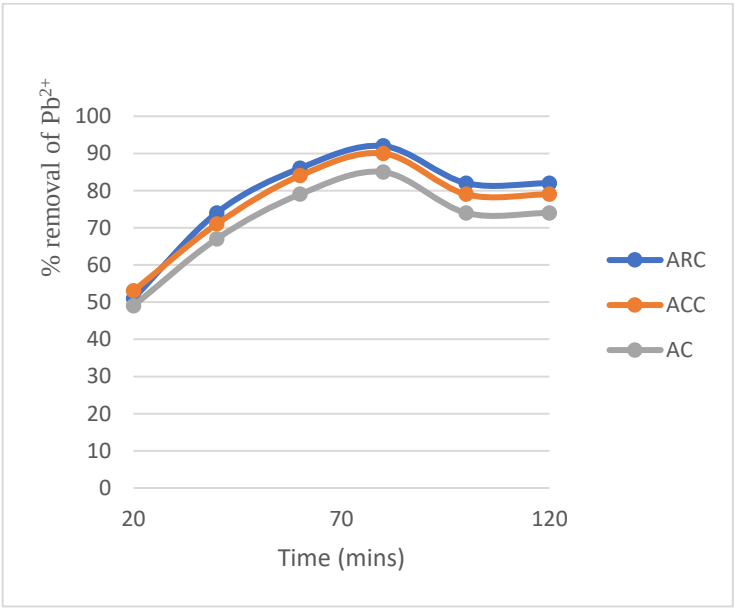

Figure 16: Effect of contact time on adsorption of Pb^{2+} with ARC, ACC and ACS

https://doi.org/10.69897

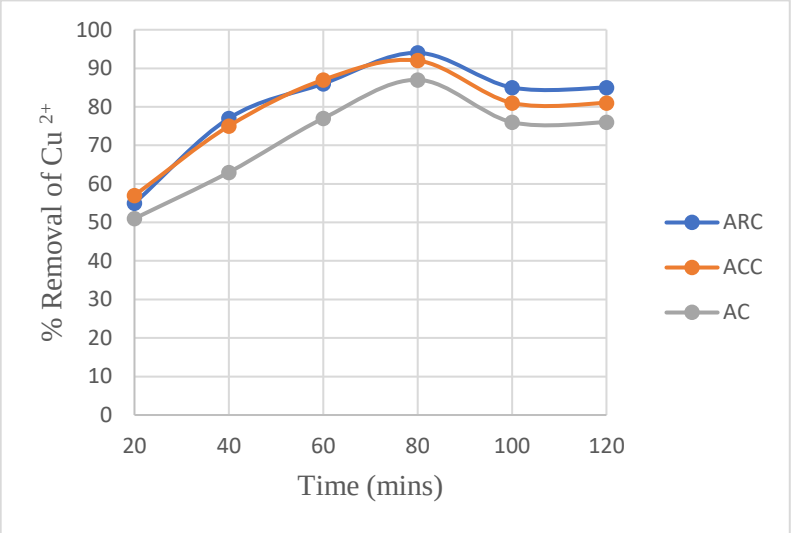

Figure 17: Effect of contact time on adsorption of Cu^{2+} with ARC, ACC and AC

The quantity of ion adsorbed into a biomass increased with time, but at some point, reached a constant value beyond which no more was removed from solution. Now, the amount of the ion desorbing from the adsorbent was in a state of dynamic equilibrium with the amount being absorbed. The quantity of ion adsorbed at the equilibrium time reflects the greatest amount of adsorption under those operating conditions. In considering the three adsorbents, ARC was a better adsorbent with a maximum adsorption percentage of 92, 94 and 96 % for Pb^{2+}, Cu^{2+} and Co^{2+}, respectively all at 80 minutes. This is attributed to its porous structure particles which enhanced adsorbent stability towards the process of taking metal ions from aqueous solutions (Srivastava *et al.,* 2017). ACC followed and the least was identified to be ACS. This trend is related to the aspect of the BET surface area which was found to be ARC>ACC>ACS. Generally, ACS is the poorest adsorbent among the three. Agglomeration of metal ions on the adsorbed surface could be the cause of the plateau stage's slow rate of adsorption (Mustapha *et al.,* 2019).

Equilibrium was reached at 60 to 80 minutes in almost all cases. The findings of this investigation are consistent with those of Rahmati *et al.* (2012). This is understandable given that, at first, there was a higher rate of ion uptake due to the high ion concentration and unoccupied sites on the adsorbent. However, as the number of adsorption sites decreased, the rate of uptake was lowered. Similar findings were reported in the Mousavi *et al.* (2010) study. The greater concentration differential between the metal ions in solution and the activated carbon surface may have contributed to the high percentage metal ion removal at lower levels of the precious timing (Afroze and Ang, 2016).

Effects of particle size and adsorbent dosage

https://doi.org/10.69897

The contact surface between any sorbent and the liquid phase plays a crucial role in sorption phenomena. For this reason, the effects of particle size of rice, coconut and clay adsorbents on removal of Cu^{2+}, Pb^{2+} and Co^{2+} ions and RB were examined utilizing three distinct sizes (100, 200 and 300 µm). The data clearly show that as the weight of the adsorbent used increased, so did the percentage of metal ions and dye that were adsorbed. It also reduced as the adsorbent's particle size increased. For every metal ion and dye in all adsorbents, the order of adsorption with particle size was 100 µm >200 µm >300 µm. This is due to the fact that smaller particle sizes directly correlate with larger surface areas, which offer more sites for improved adsorption capacity (Wang and Shadman, 2013). Adsorption rate rises as mesopore volume increases and particle size decreases (Muller, 2010).

Comparing the adsorption rate of 100 µm particle size for all adsorbents revealed the order ARC >ACC >ACS as shown in **Figures 18** to **20**. In all adsorbents Co^{2+} ion was the most adsorbed which could be due to its small size as compared to other adsorbates (Bao *et al.,* 2024). The order of how adsorbates were adsorbed was Co^{2+}>Cu^{2+}>RB>Pb^{2+}.

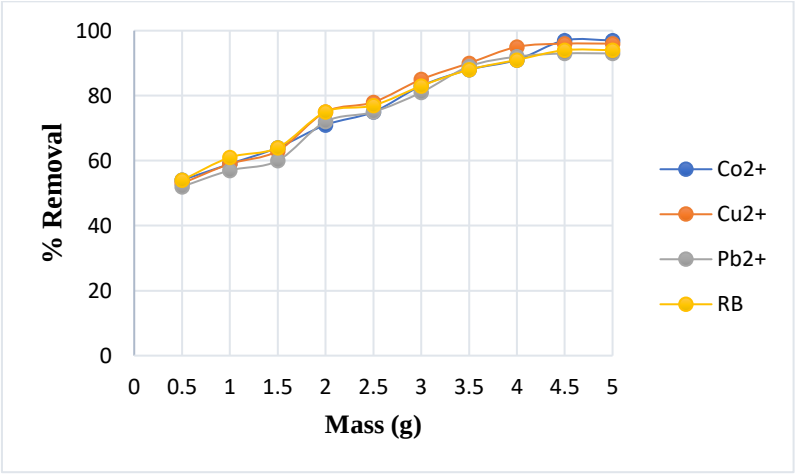

Figure 18: Adsorption effect of 100 µm ARC particle size and dosage on RB and metal ions

https://doi.org/10.69897

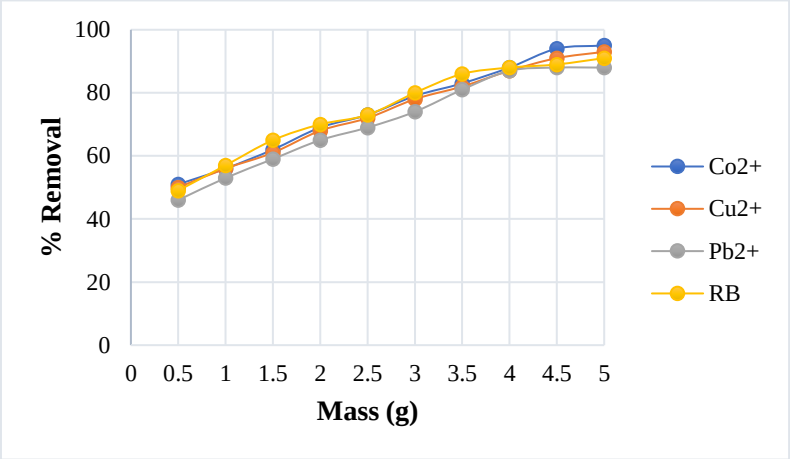

Figure 19: Adsorption effect of 100 µm ACC particle size and dosage on RB and metal ions

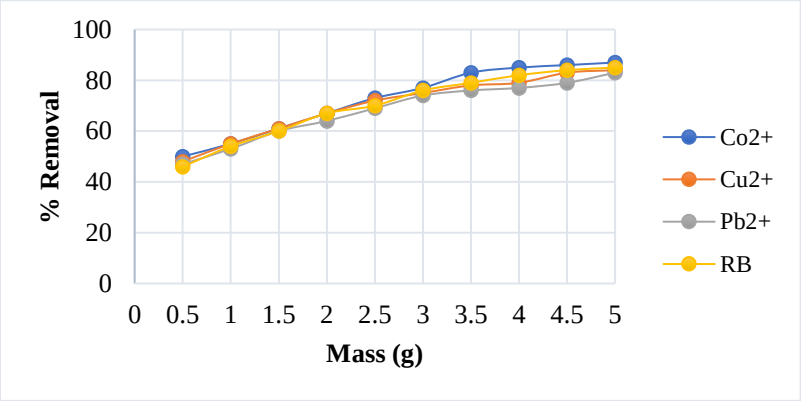

Figure 20: Adsorption effect of 100 µm ACS particle size and dosage on RB and metal ions

Conclusion

According to the results of this study, ARC, ACC, and ACS can be employed as natural, viable and cost-effective adsorbents for removing RB dye and Co^{2+}, Cu^{2+}, and Pb^{2+} ions from aqueous solutions. Using BET, XRD, and FTIR, the surface area, phase identification, and functional groups in charge of removing dye and metal ions from aqueous solutions were investigated. Contact time, size, dosage, solution pH, and temperature all affect the batch adsorption process. The findings suggest that agricultural and natural wastes such as rice husks, coconut shells, and clay soil can be repurposed into cost-effective materials for wastewater treatment in developing regions. The adsorption effect for the adsorbents revealed the order ARC >ACC >ACS for all metal ions in study and the dye.

Recommendations

The aforementioned conclusions and findings suggest additional research on the following topics:

i. It is important to look into how effective ARC, ACC, and ACS are at removing different kinds of contaminants, such as pesticides, other inorganic pollutants, organic pollutants, and pharmaceutical waste effluents.
ii. It is necessary to test the biosorbents in the study to see if they can remove heavy metal ions from actual water samples.
iii. Using various ratios, a comparative analysis of the efficacy and efficiency of rice husk, coconut shells, clay, and other biomass should be conducted.
iv. Studies on adsorbents used if they can be recyclable using a suitable regenerating agent to make the process more economical.
v. Evaluating the adsorbents' applicability for industrial and municipal water treatment applications by scaling up from laboratory batch studies to continuous-flow column trials.
vi. Conducting life-cycle and economic feasibility analyses to ascertain the commercial viability, environmental impact, and cost-effectiveness of manufacturing and utilizing these biosorbents on a broad scale.
vii. Investigating the possibility of recovering adsorbed heavy metals from wasted adsorbents for resource recovery and secure disposal, hence promoting circular economy wastewater treatment strategies.
viii. Investigation of hybrid treatment systems that combine adsorption with additional methods (such as coagulation, photocatalysis, and membrane filtering).

References

Abdulredha, M., Rafid, A., Jordan, D. and Hashim, K. (2017). The development of a waste management system in Kerbala during major pilgrimage events: determination of solid waste composition. *Procedia Engineering;* **196**: 779–784. https://doi.org/10.1016/j.proeng.2017.08.007

https://doi.org/10.69897

Afroze, S., Sen, T.K. and Ang, H.M. (2016). Adsorption removal of zinc (II) from aqueous phase by raw and base modified Eucalyptus sheathiana bark: Kinetics, mechanism and equilibrium study. *Process Safety and Environmental Protection*, **102**: 336-352. https://www.sciencedirect.com/science/article/abs/pii/S095758201630026X

Al-Hashimi, O., Hashim, K., Loffill, E., Marolt, C. T., Nakouti, I., Faisal, A. A. and Al-Ansari, N. (2021). A comprehensive review for groundwater contamination and remediation: occurrence, migration and adsorption modelling. *Molecules;* **26**(19):5913. https://doi.org/10.3390/molecules26195913

Al-Sareji, O. J., Grmasha, R. A., Salman, J. M., Idowu, I. and Hashim, K. S. (2021). Street dust contamination by heavy metals in Babylon governorate, Iraq. *Journal of Engineering Science and Technology;* **16**(1):3528–3546. https://researchonline.ljmu.ac.uk/id/eprint/17033/

Argun, M. E., Dursun, S., Ozdemir, C., and Karatas, M. (2006). Heavy metal adsorption by modified oak sawdust: Thermodynamics and kinetics. *Journal of Hazardous Materials*, **141**, 77–85. https://doi.org/10.1016/j.jhazmat.2006.06.095

Bakti, A. I. and Gareso, P. L. (2018). Characterization of Active Carbon Prepared from Coconuts Shells Using FTIR, XRD and SEM Techniques. *Jurnal ilmiah pendidikan fsika Al-Biruni* **7**:33-39. https://ejournal.radenintan.ac.id/index.php/al-biruni/article/view/2459

Bao, J., Feng,Y., Pan,Y. and Jiang, J. (2024). Adsorption of Co^{2+} and Cr^{3+} in Industrial. Wastewater by Magnesium Silicate Nanomaterials. *Materials,* **17**(9): 1746. https://www.mdpi.com/1996-1944/17/9/1946

Chengo, K., Murungi, J. and Mbuvi, H. (2013). Speciation of Zinc and Copper in Open-Air Automobile Mechanic Workshop Soils in Ngara Area-Nairobi Kenya. *Resources and Environment*, **3:** 145-154.

Ewecharoena, A., Thiravetyana, P. and Bertagnollib, H. (2009). Nickel adsorption by sodium polyacrylate-grafted activated carbon. *J. Haar. Mat*, **171**:335-339. https://doi.org/10.1016/j.jhazmat.2009.06.008

Fu, F. and Wang, Q. (2011). Removal of heavy metal ions from wastewaters: A review. *Journal of Environmental Management*, **92,** 407–418. https://doi.org/10.1016/j.jenvman.2010.11.011

Ghanadzadeh, A., Zanjanchi, M.A. and Tirbandpay, R. (2002). The role of host environment on the aggregative properties of some ionic dye materials, *J. Mol. Struct*. **616**: 167-174. https://www.sciencedirect.com/science/article/abs/pii/S0022286002003241

Gong, R., Ding, Y., Liu, H., Chen, Q. and Liu, Z. (2005). Lead biosorption by intact and pretreated Spirulina maxima biomass. *Chemosphere*, **58:** 125-130. https://doi.org/10.1016/j.chemosphere.2004.08.055

Gupta N, Kushwaha AK, Chattopadhyaya, M. C. (2012). Adsorption studies of cationic dyes onto Ashoka (*Saraca asoca*) leaf powder. *J. Taiwan Inst Chem Eng*, **43**:604–613. https://doi.org/10.1016/j.jtice.2012.01.008

Hui, K. S., Chao, C. Y. H., and Kot, S. C. (2005). Removal of mixed heavy metal ions in wastewater by zeolite and residual products from recycled coal fly ash. *Journal of Hazardous Materials*, **127:** 89–101. https://doi.org/10.1016/j.jhazmat.2005.06.027

Irannajad, M. and Haghighi, H. K. (2017). Removal of Co^{2+}, Ni^{2+} and Pb^{2+} by manganese oxide-coated zeolite: Thermodynamics and kinetic studies. Clays and clay minerals. **65**: 52-62. https://www.cambridge.org/core/journals/clays-and-clay-minerals/article/abs/removal-of-co2-ni2-and-pb2-by-manganese-oxidecoated-zeolite-equilibrium-thermodynamics-and-kinetics-studies/C27423F17872D43F833414894400F667

Katircioğlu, H., Aslim, B., Türker, R. A., Atici, T., and Beyatli, Y. (2008). Removal of cadmium(II) ion from aqueous system by dry biomass, immobilized live and heat inactivated Oscillatoria sp. H1 isolated from freshwater (Mogan Lake). *Bioresource Technology*, **99:** 4185–4191. https://www.sciencedirect.com/science/article/abs/pii/S0960852407007316

Khan, A., Naqvi, H. J., Afzal, S., and Jabeen, S. (2017). Efficiency Enhancement of Banana Peel for Waste Water Treatment through Chemical Adsorption. *Academy of Sciences: A. Physical and*

https://doi.org/10.69897

Computational Sciences, **54**(3), 329–335. http://ppaspk.org/index.php/PPAS-A/article/view/230

Kobya, M., Demirbas, E., Senturk, E., Ince, M. (2005). Adsorption of heavy metal ions from aqueous solutions by activated carbon prepared from apricot stone, *Bioresource Technology*, 96 **13**, 1518–1521. https://www.sciencedirect.com/science/article/abs/pii/S0960852405000039

Levin, R., Brown, M. J., Kashtock, M. E., Jacobs, D. E., Whelan, E. A., Rodman, J., and Sinks, T. (2008). Lead exposures in US children, 2008: implications for prevention. *Environmental Health Perspectives*, **116:** 1285. https://doi.org/10.1289/ehp.11241

Manyangadze, M., Chikuruwo, N. M. H., Narsaiah, T. B., Chakra, C. S., Charis, G., Danha, G., and Tirivaviri, A. M. (2020). Adsorption of lead ions from wastewater using nano silica spheres synthesized on calcium carbonate templates. *Heliyon*, **6**(11): 1–13. https://www.cell.com/heliyon/fulltext/S2405-8440(20)32152-6

Mousavi, H. Z., Hosseynifar, A., Jahed, V. and Dehghani, S. A. (2010). Removal of Lead from Aqueous Solution using Waste Tire Rubber Ash as an Adsorbent. Brazilian Journal of Chemical Engineering, **27**(01): 79–87. https://www.scielo.br/j/bjce/a/9fjbLB3Yg7hHJKXjkhnsxQS/?format=html&lang=en

Muiruri, J., Nyambaka, H. and Ngwiri, M. (2013). Heavy metals in water & tilapia from Athi Galana-sabaki tributaries Kenya. *International Food Research Journal*, **20:** 891-896. https://ir-library.ku.ac.ke/server/api/core/bitstreams/8cd6bb63-cadc-4b8e-b9f9-9b5ea553d3f9/content

Muller, B. R. (2010). Effect of particle size and surface area on the adsorption of albumin- bonded bilirubin on activated carbon. *Elsevier*, **48:** 3607-3615. https://www.sciencedirect.com/science/article/abs/pii/S0008622310004045

Mustapha, S., Shuaib, D. T., Ndamitso, M. M., Etsuyankpa, M. B., Sumaila, A., Mohammed, U. M., & Nasirudeen, M. B. (2019). Adsorption isotherm, kinetic and thermodynamic studies for the removal of Pb (II), Cd (II), Zn (II) and Cu (II) ions from aqueous solutions using Albizia lebbeck pods. *Applied water science*, *9*(6), 142.

Naja, G., Mustin, C., Berthelin, J. and Volesky, B. (2010). Lead biosorption study with *Rhizopus arrhizus* using a metal-based titration technique. *J Colloid and Interface Science.* **292**(2):537–543. https://doi.org/10.1016/j.jcis.2005.05.098

Ngah, W.W. and Hanafiah, M. M. (2008). Removal of heavy metal ions from wastewater by chemically modified plant wastes as adsorbents: a review. *Bioresource technology*, **99**(10): 3935–3948. https://doi.org/10.1016/j.biortech.2007.06.011

Pang, T., Yang Z., Huang, Y., Lei, X., Zeng, X., Li, X. (2018). Adsorption Properties of Thiol Modified, Sodium-Modified and Acidified Bentonite for Cu^{2+}, Pb^{2+} and Zn^{2+} *Spectrosc. Spectr. Anal.* **38**:1203–1208.

Rahmati, A., Ghaemi, A. and Samadfam, M. (2012). Kinetic and Thermodynamic studies of Uranium(VI) Adsorption Using Amberlite IRA-910 Resin. *Annals of Nuclear Energy*. **39**: 42-48. https://doi.org/10.1016/j.anucene.2011.09.006

Salah, Z. L., Gharghan, S. K., Dooley, J., Alkhaddar, R. M. and Abdellatif, M. (2018). Short term urban water demand prediction considering weather factors. *Water Resource Management;* **32**(14): 4527–4542. https://link.springer.com/article/10.1007/s11269-018-2061-y

Sheta, A., Falatah, M., Sewailem, S., Khaled, E. and Sallam, H. (2003). Sorption characteristics of zinc and iron by natural zeolite and bentonite. *Microporous Material*, **61:** 127-136. https://doi.org/10.1016/S1387-1811(03)00360-3

Srivastava, V., Shekhar, M., Gusain, D., Gode, F., and Sharma, Y. C. (2017). Application of a heterogeneous adsorbent (HA) for the removal of hexavalent chromium from aqueous solutions: Kinetic and equilibrium modeling. *Arabian Journal of Chemistry*, **10**: 1–26. https://www.sciencedirect.com/science/article/pii/S187853521300419X

https://doi.org/10.69897

Tong, S., Schirnding, Y., Von, E. and Prapamontol, T. (2000). Environmental lead exposure: a public health problem of global dimensions. *Bulletin of the World Health Organization*, **9:** 1068-1077. https://www.scielosp.org/pdf/bwho/v78n9/v78n9a03.pdf

Ugwu, E. I., Tursunov, O., Kodirov, D., Shaker, L. M., Al-Amiery, A. A., Yangibaeva, I. and Shavkarov, F. (2020). Adsorption mechanisms for heavy metal removal using low cost adsorbents: A review. *IOP Conference Series: Earth and Environmental Science*, **614**(1): 1–13.

Vieira, M. G. A., De-Almeida, N. A. F., Da-Silva, M. G. C., Carneiro, C. N. and Melo, F. A. (2013). Adsorption of Lead and Copper Ions from Aqueous Effluents on Rice Husk Ash in a Dynamic System. *Brazilian Journal of Chemical Engineering,* **31**(2):519 – 529. https://www.scielo.br/j/bjce/a/PHmwC7VKH6xFnpWMG4rDv8k/?lang=en

Wang, H. and Shadman, F. (2013). Effect of particle size on the adsorption properties of oxide nanoparticles. American institute of chemical engineers, **59**(5): 1502-1510. https://doi.org/10.1002/aic.13936

Winter, M. & Brodd, R. J. (2004). What Are Batteries, Fuel Cells, and Supercapacitors? *Chem. Rev.* **104**: 4245–4270. https://pubs.acs.org/doi/full/10.1021/cr020730k

Yagub, M. T., Sen, T. K., Afroze, S. and Ang, H. M. (2014). Dye and its removal from aqueous solution by adsorption: a review. *Advances in Colloid and Interface Science;* **209**:172–184. https://doi.org/10.1016/j.cis.2014.04.002

Zhao, H. and Lang, Y. (2018). Adsorption behaviors and mechanisms of florfenicol by magnetic functionalized biochar and reed biochar. *Journal of the Taiwan Institute of Chemical Engineers*, **88**: 152-160. https://doi.org/10.1016/j.jtice.2018.03.049